Reorganization and Melting of Polyethylene Single Crystals: Complementary TEM, DSC, and Real-Time AFM Studies

Sally J. Organ,*,† Jamie K. Hobbs,‡ and Mervyn J. Miles§

Department of Materials Engineering, The Open University, Walton Hall, Milton Keynes MK7 6AA, UK; Department of Chemistry, University of Sheffield, Brook Hill, Sheffield, S3 7HF; and H H Wills Physics Laboratory, University of Bristol, Tyndall Avenue, Bristol BS8 1TL, UK

Received December 19, 2003; Revised Manuscript Received April 21, 2004

ABSTRACT: The reorganization and melting of single crystals of linear polyethylene with lozenge and truncated-lozenge habits has been studied in situ during slow continuous heating using atomic force microscopy. The morphological insights obtained are backed up by complementary experiments using transmission electron microscopy and differential scanning calorimetry and have enabled us to identify different stages of melting/recrystallization. Visible melting is preceded by local reorganization within the crystals, the extent of which depends crucially on the thermal history of the sample and can influence subsequent behavior such as the preferential melting of one crystal sector before another. This is followed by distortion of the crystal edges and limited thickening which does not progress into the bulk of the crystal. Next, larger scale melting and recrystallization occurs within the bulk of the crystal, which leads to a progressive increase in melting point. The observed behavior supports a model of local melting and recrystallization rather than solid-state thickening, and overlying layers can behave quite independently. Finally, the thickened crystals melt at a temperature dependent on the thermal history of the sample.

Introduction

When polymers are crystallized from either the melt or solution, they have a supercooling-dependent thickness, the general consensus being that this thickness is controlled by the kinetics of crystal growth[1] rather than equilibrium considerations.[2] Subsequent annealing leads to a reorganization and thickening of the crystal as it tries to obtain its equilibrium extended (or nearer to extended[3]) chain conformation. The details of this crystal reorganization have been the subject of study for many years, and it remains unclear the extent to which a solid state or melting and recrystallization process dominates. In many studies solution grown single crystals have been used as a model system to understand the thickening of polymer lamellae in general,[4] with the rationale that it should be more straightforward to discern the difference between processes.

As well as the question of how the process of crystal thickening occurs, there has also been considerable interest in how polymers melt. This is an interesting question both on a fundamental level—what do we mean thermodynamically by melting when applied to crystals that are clearly far from equilibrium[5]—and, practically, on if melting occurs spontaneously everywhere once a particular temperature is obtained or if it is a nucleated process.[6] Recently, these issues have been the subject of increased interest as attention has shifted toward the possible role of metastable states during crystallization[7] and to new insights into melting behavior obtained from modern X-ray scattering techniques and analysis.[8]

In polyethylene the issue is further complicated by the presence of different structures within a single crystal, when the crystal "fold surfaces" are considered. When polyethylene crystallizes slowly from dilute solution, it is usually assumed that the molecules lay down on the growth front layer by layer, each molecule folding back into approximately the adjacent lattice site along a particular crystallographic plane. In the case of polyethylene the 110 and 100 growth fronts grow at comparably slow rates, the relative rates depending on crystallization temperature.[9] This leads to the formation of either lozenge-shaped crystals, with 110 lateral faces, or truncated lozenges, with both 110 and 100 faces. As the "folding" direction is different along the different growth fronts, this leads to the sectorization of the crystal into regions with clearly different "fold" surfaces. A difference in melting point between these sectors was first reported by Bassett and Keller[10] and is discussed in ref 11. Several other studies have been carried out on the melting of crystals containing different proportions of 110 and 100 sector, some of which have reported a difference in melting temperature between the sectors [e.g., ref 12 and some examples in ref 13] and some of which have not [e.g., ref 14 and other examples in ref 13].

The aim of the work reported here was to use the relatively new technique of atomic force microscopy (AFM) to study the reorganization of single crystals of polyethylene in situ, in real time, and directly observe the melting behavior. AFM has been used recently by several groups to study the reorganization of single crystals of polyethylene both in situ and ex situ, sometimes in combination with other techniques [e.g., refs 15−19]. Here we combine the AFM study with experiments using transmission electron microscopy (TEM) and differential scanning calorimetry (DSC). Each of these techniques can provide different but complementary information. DSC gives precise calorimetric data averaged over a relatively large sample volume. Melting temperatures and relative heats can

† The Open University.
‡ University of Sheffield.
§ University of Bristol.
* Corresponding author.

10.1021/ma035955r CCC: $27.50
Published on Web 05/20/2004

be precisely defined. TEM gives real-space information comparable to that obtained by AFM, but, because it is a fast technique, it is possible to obtain good sample statistics. AFM allows the process to be imaged as it happens, as, if care is taken, the degree of interaction with the material that is being imaged can be minimal. However, AFM is slow so the sample statistics tend to be relatively limited. Thus, by combination of these techniques, we hope to obtain a relatively complete picture of what is occurring. In this work (and in contrast to other similar studies) we have paid particular attention to the influence of heating rate or prior annealing on the subsequent melting behavior and have shown this to be a crucial factor.

Some caution is required when comparing results from the two experimental methods. We are primarily concerned with crystal behavior and morphology at high temperature during the melting process. We have therefore chosen not to include AFM measurements from cooled crystals, since the molten material will have recrystallized during cooling and is unlikely to be representative of the high-temperature state. The TEM micrographs, however, were obtained after the crystals have been cooled, and some of the visible structure will have emerged during this process: the UHV conditions used for TEM imaging may also lead to structural changes of the annealed samples. Finally, the presence of a substrate may influence the structural changes that occur during heating in the AFM. All these factors warrant further investigation but are outside the scope of the current paper.

Experimental Details

Polyethylene single crystals were grown using the self-seeding technique[19] to produce small and uniform crystals. Lozenge-shaped crystals were grown from a 0.1% solution of nascent (as-polymerized) Rigidex 50 ($M_w \approx 100\,000$, $M_w/M_n \approx 10$) in *p*-xylene, using a seeding temperature of 99.0 °C and a crystallization temperature of 70.0 °C for 3.5 h. Truncated lozenge-shaped crystals were grown from a 0.05% solution of nascent Rigidex 50 in octane, using a seeding temperature of 107.5 °C and a crystallization temperature of 93.0 °C for 4 h. In both cases the suspensions were hot-filtered and the crystals washed with solvent at the crystallization temperature to remove any polymer remaining in solution and thus to prevent the formation of thinner rims around the crystals during cooling. Crystals were deposited onto carbon-coated grids and shadowed with Pt/Pd for examination by TEM.

Sectorization within the crystals was revealed by evaporating polyethylene onto the surface of crystals deposited onto carbon coated grids[20] and shadowing with Pt/Pd.

For DSC melting studies the original solvent was exchanged for silicone oil. This ensures that the crystals remain isolated during melting. Small quantities of the suspension were sealed into aluminum volatile sample pans, and the melting behavior was recorded at heating rates between 1 and 40 °C min^{-1}. For some samples heating was stopped at a fixed point during the melting cycle, and after cooling, the partially melted crystals were extracted from the silicone oil for TEM examination. This enabled correlation between particular DSC melting peaks and changes in crystal morphology. In a few cases parallel samples were prepared by heating crystals deposited onto carbon-coated grids in a microscope hot stage to an equivalent temperature to that used in the DSC: the two techniques produced very similar results, but the DSC method was felt to give a more unambiguous association between melting temperature and morphology.

Annealing experiments were carried out by holding samples for short times at temperatures just below, or within, the range of melting temperatures. After annealing, the samples were cooled to 100 °C before reheating to melt. The cooling step allows the DSC to equilibrate so that clear melting peaks are subsequently obtained. The temperatures and rates employed are described below.

For AFM experiments, a drop of suspension was deposited onto a glass cover slip and the solvent evaporated. A Veeco Dimension D3100 was used in Tapping Mode using standard silicon cantilevers with a nominal spring constant of 50 N m^{-1} and a resonant frequency of approximately 250 kHz. The temperature of the sample was controlled using a Linkam heater, using the same experimental setup as described in ref 21. The accurate measurement of the temperature of the sample surface is influenced by the distance from the heat shield, the alignment of the probe relative to its holder, and other factors that vary from experiment to experiment, making a reliable calibration problematic. The final melting temperature of the crystals was used to calibrate against the DSC data. The temperatures quoted are corrected using this correction factor. Although the absolute temperature calibration may be subject to an uncertainty of the order of ±1 °C, the relative temperatures within a series of images are accurate and are therefore quoted to 0.1 °C.

Topography images were collected on both trace and retrace (that is, as the probe is moving from left to right and then when the probe is moving from right to left). At the high scan rates used, some degradation in image quality as the probe passes over a high point in the sample occurs. This poor tracking of the surface will occur on opposite sides of the feature for the trace and retrace of each line, so the correct position and shape of the feature can be determined more accurately by a comparison of these two images. Phase images were also collected, which provide additional information about the material properties being imaged. Under the imaging conditions used for these studies, hard materials appear light, while sticky and soft materials appear dark, giving a contrast between crystalline and amorphous material. Phase images also contain increased contrast at edges due to the finite time allowed for the microscope feedback to respond. In the images shown these can be seen as a lighter region if the edge steps up as approached from the left and a dark region if the edge steps down as approached from the left. These localized edge effects are artifacts of the imaging technique and do not indicate a change in material properties at the edges.

For the AFM experiments the samples were either heated at a continuous rate of 1 °C min^{-1} or heated at this rate but then held intermittently at constant temperature to allow the changes to be followed isothermally. The average heating rate of the crystals in the AFM experiments was therefore somewhat slower than even the slowest rate used in the DSC. Images were taken continuously; a complete scan taking between 30 and 60 s, depending on the scan area. In experiments when the sample is being heated, there is a constant drift in the sample position due to the thermal expansion of the heater stage. As the image is built up line by line, this leads to a either a slight stretching or slight contraction of the image depending on the scan direction (i.e., building up the image line by line starting from the bottom or starting from the top). This leads to the size of the crystal appearing to change slightly depending on scan direction.

Results

Figure 1 shows typical examples of the lozenge (Figure 1a) and truncated lozenge (Figure 1b) shaped crystals. Polyethylene decoration has been used to reveal the sectorization within the truncated lozenge crystals. The basic lozenge-shaped crystals contain four (110) sectors; the truncated lozenges also have very pronounced (100) sectors making up approximately 38% of the total crystal volume.

The DSC traces in Figures 2 and 3 show how the melting behavior varies according to heating rate. Two main melting endotherms are obtained as well documented previously [e.g., ref 13]. The first peak, between approximately 120 and 126 °C, corresponds to melting

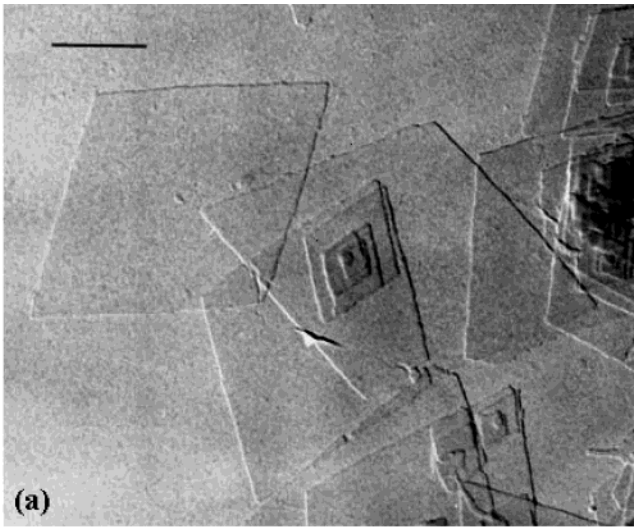

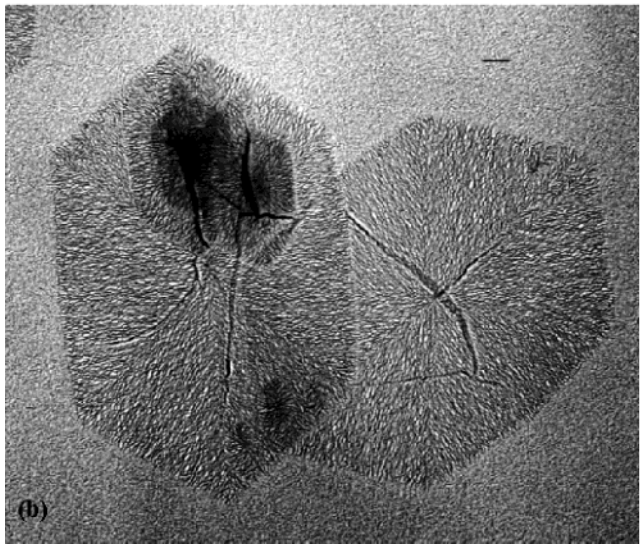

Figure 1. Polyethylene single crystals used for melting studies. (a) Lozenge-shaped crystals. Marker = 0.2 μm. (b) Truncated lozenge crystals decorated with polyethylene to reveal sectorization. Marker = 1 μm.

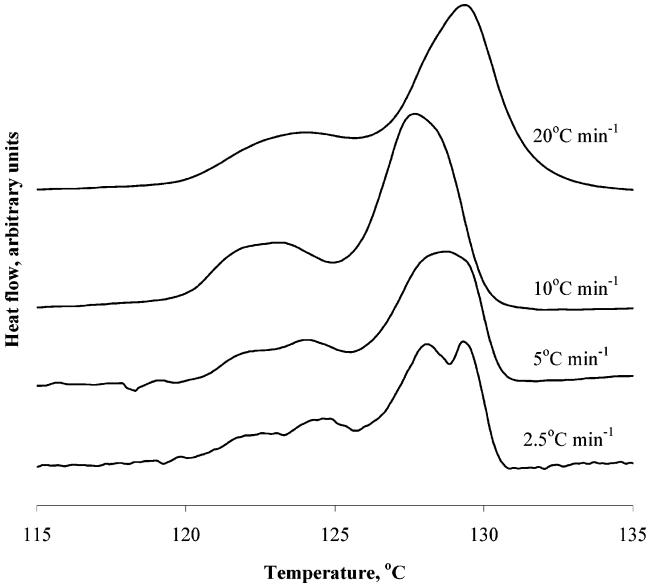

Figure 2. Melting endotherms for lozenge-shaped crystals, obtained at the heating rates shown. The heat flow values have been normalized for heating rate.

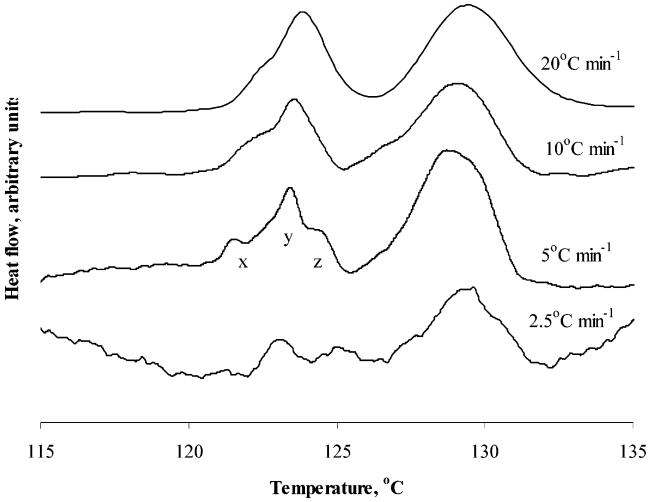

Figure 3. Melting endotherms for truncated lozenge crystals, obtained at the heating rates shown. The heat flow values have been normalized for heating rate. See text for discussion of peaks x, y, and z.

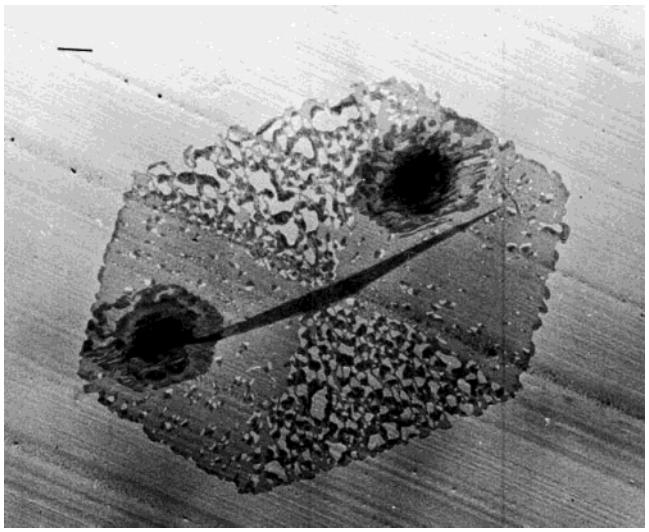

Figure 4. Truncated lozenge crystal heated at 20 °C min^{-1} to 123 °C and then cooled. Marker = 1 μm.

and annealing of the original crystals. The second peak, between approximately 127 and 132 °C, corresponds to melting of the annealed material. Although peak positions have been corrected for heating rate using an indium calibration, some thermal lag in the sample is still apparent from the slightly higher peak positions obtained at higher rates. Subsidiary structure can occur within both peaks and is dependent on heating rate. In this work only the initial peak, and the subsidiary structure within it, is of interest, and it should be assumed that all subsequent description and discussion refer to this peak alone.

Preferential Sector Melting. Some previous studies of single crystal melting [e.g., ref 13] have reported a split melting peak for truncated lozenges, which can be associated with the successive melting of the different crystal sectors. There are many examples of split melting peaks in Figures 2 and 3, but these could only be correlated with early melting of the (100) sectors when truncated lozenges were heated at the higher heating rates of 10 and 20 °C min^{-1}. Figure 4 shows an electron micrograph of such crystals that have been heated to 123 °C, the temperature of the low-tempera-

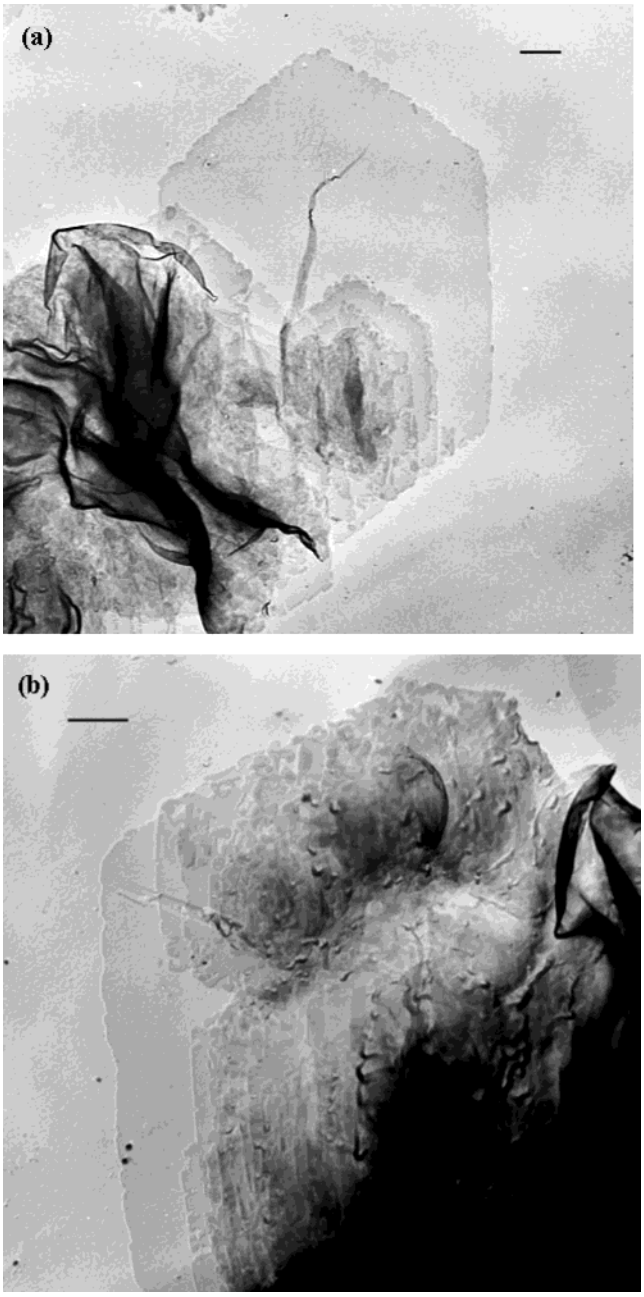

Figure 5. Electron micrographs showing truncated lozenge crystals heated at 5 °C min^{-1} to (a) 122 °C and (b) 124 °C. Markers = 1 μm.

ture shoulder, and then cooled. The (100) sectors have completely melted, while the (110) sectors are largely intact except at the edges. It is clear that the (100) sector has melted prior to, and separately from, the (110) sector, in line with previous observations on similar crystals.

However, clear preferential sector melting was not observed at the lower heating rates utilized in the AFM, and the multiple DSC peaks obtained when the heating rate is 5 °C min^{-1} or less (labeled x, y, and z in Figure 3) were found not to be associated with preferential sector melting. Figure 5 shows TEM images of crystals extracted after heating to 122 °C (between peaks x and y) and 124 °C (between peaks y and z). There is no evidence of preferential sector melting here, nor was any seen in crystals heated at lower rates.

The melting behavior was also affected by annealing truncated lozenge crystals at temperatures just below

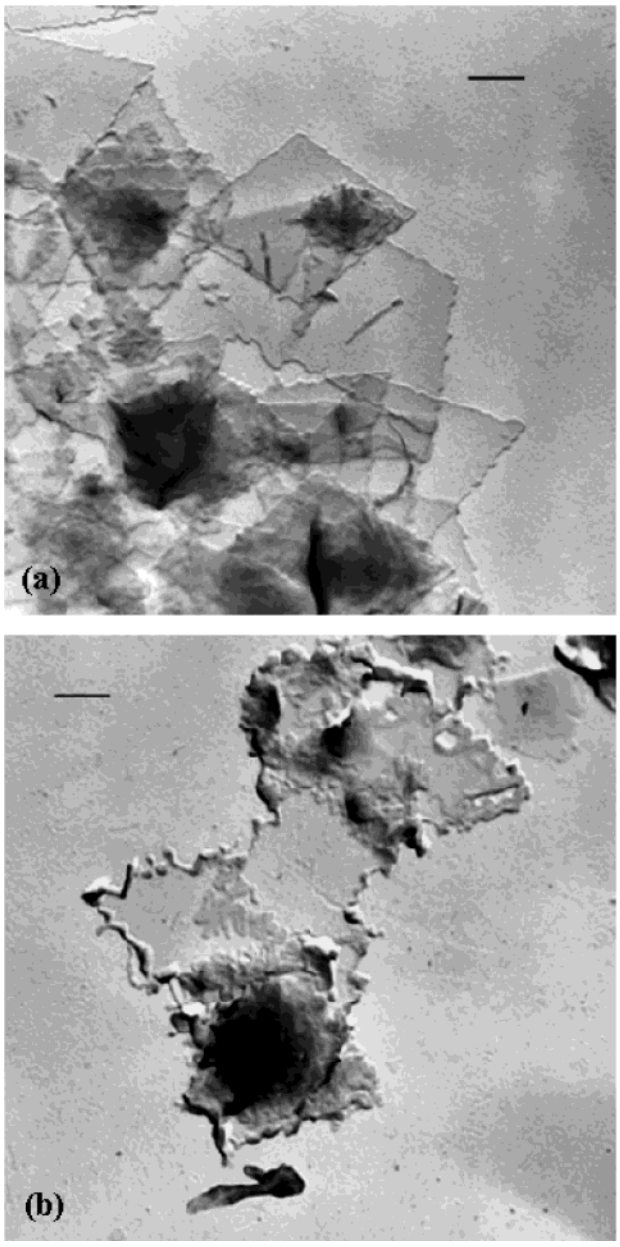

Figure 6. Lozenge-shaped crystals heated to (a) 121 °C and (b) 123 °C. Markers = 0.2 μm.

the lowest visible melting peak. Annealing for 10 min at temperatures in the range 115−118 °C caused subtle changes in the subsequent melting behavior: crystals held for 10 min at 118 °C and subsequently melted at 10 °C min^{-1} produced a melting trace very similar to that initially recorded at 5 °C min^{-1} for unannealed crystals. It therefore appears that changes are taking place within the crystals at temperatures below the apparent onset of melting, which affect the subsequent melting/annealing behavior. One consequence of this is that preferential sector melting is not observed at low heating rates.

Morphological Changes during Melting. Lozenge-shaped crystals suspended in silicone oil were heated at 5 °C min^{-1} to 121, 123, and 125 °C and then extracted for examination by TEM. By comparison with Figure 2, it can be seen that these temperatures correspond to the onset, midpoint, and end point of the initial melting peak. Parts a and b of Figure 6 show crystals extracted at 121 and 123 °C, respectively. Reorganization begins

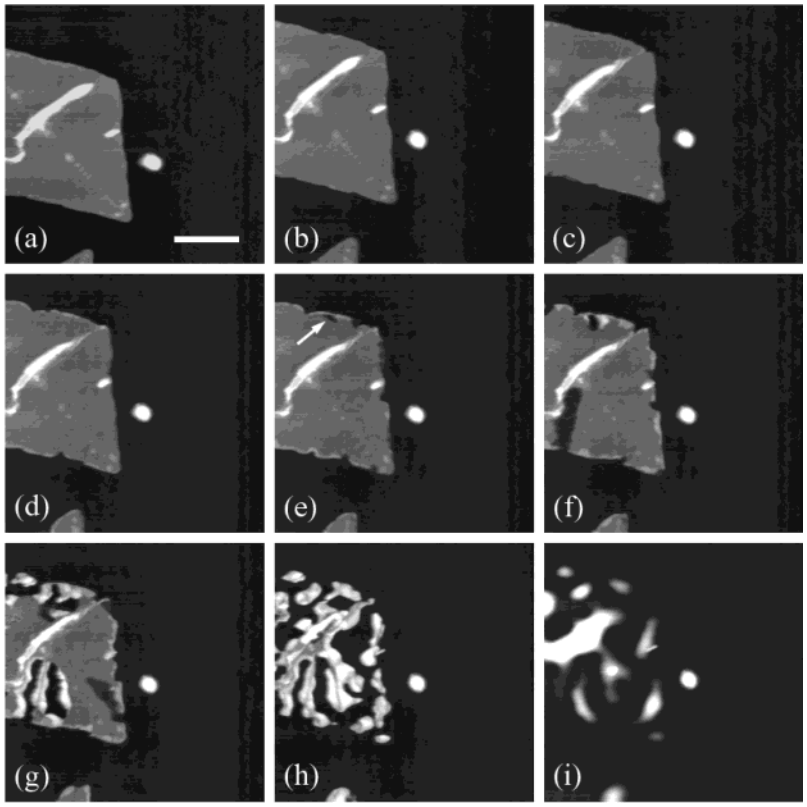

Figure 7. A series of AFM topographic images showing the thickening of lozenge-shaped crystals. Black to white represents a change in height of 50 nm. The scale bar represents 1 μm. See text for details of temperature calibration. (a) 104 °C, 0 s; (b) 116.3 °C, 806 s; (c) 118.1 °C, 915 s; (d) 119.7 °C, 1315 s; (e) 121.6 °C, 1598 s; (f) 122.5 °C, 1707 s; (g) 123.4 °C, 1816 s; (h) 127.1 °C, 2265 s; (i) 131.7 °C, 2538 s.

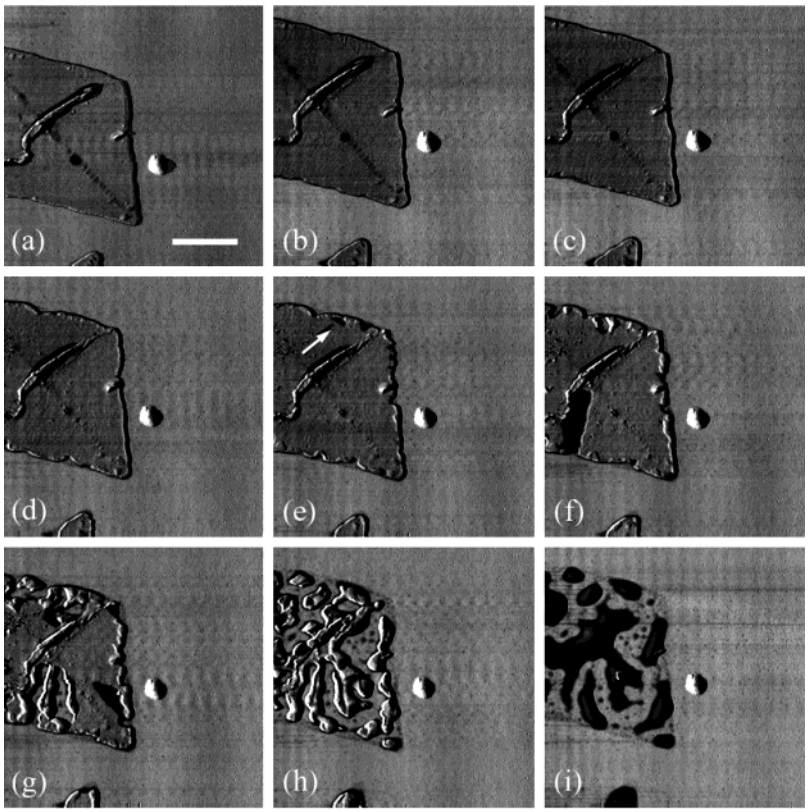

Figure 8. A series of AFM phase images collected simultaneously with the topographic images shown in Figure 7.

at the edges of the crystals: the edges appear serrated on all sides and include patches of thicker crystal. At this temperature no changes are seen in the interior of the monolayer crystals. In Figure 6b, the melting which started at the edges has extended back into the crystals, and a few holes have begun to appear in the interior; these holes are surrounded by thickened material. From the TEM experiments it is not possible to determine

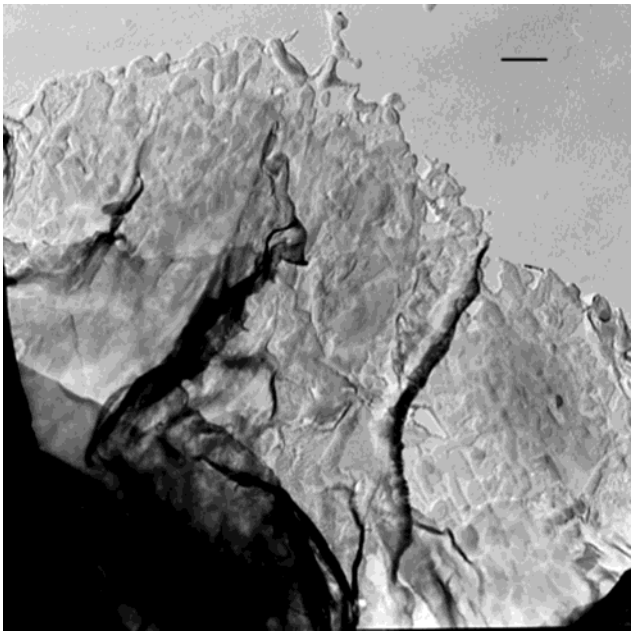

Figure 9. Truncated lozenge crystal heated to 124 °C at 2.5 °C min^{-1}. Marker = 1 μm.

whether the thickened material was produced during the initial heating or deposited on subsequent cooling. No recognizable crystals could be recovered after heating to 125 °C, confirming that the second (set of) melting peak(s) is derived from the melting of thickened material.

Figures 7 and 8 show a sequence of AFM images (topography and phase, respectively) from lozenge-shaped crystals heated over a similar range of temperature, which show the same general pattern of behavior. The AFM images reveal noticeable distortion in the crystal shape before any visible melting takes place (Figure 7a). Patches of thicker crystal then begin to appear around the crystal edges, and some rearrangement occurs (Figure 7b−d). Crystals could be held isothermally for considerable times at this stage without any further progression of melting into the bulk of the crystal.

Continued heating causes further changes. In Figure 7e we see a crystal substantially, but not completely, bounded by a thicker rim. This rim does not prevent crystal from melting behind it—the top edge of the crystal has two large indentations and also a molten patch in the interior (arrowed), completely bounded by

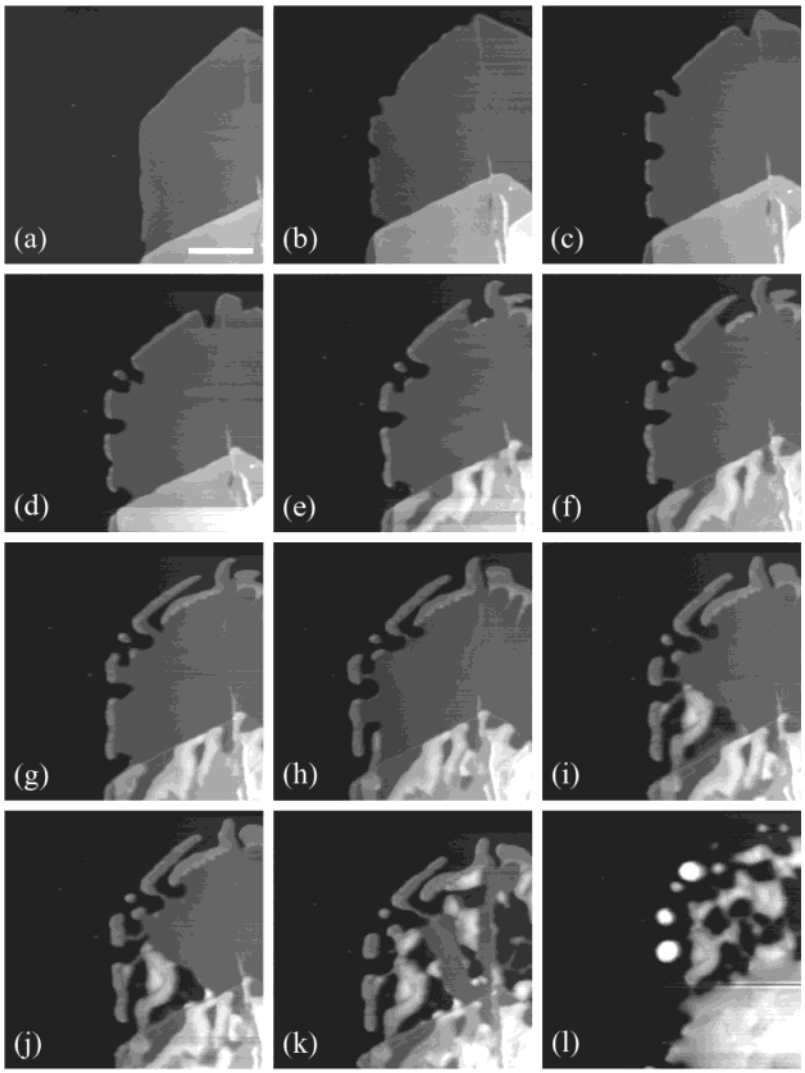

Figure 10. A series of AFM topographic images showing the thickening of truncated lozenge-shaped crystals. Black to white represents a change in height of 100 nm. Scale bar represents 1 μm. See text for details of temperature calibration. (a) 109.6 °C, 0 s; (b) 120.71 °C, 894 s; (c) 122.2 °C, 1590 s; (d) 123.6 °C, 1989 s; (e) 124.6 °C, 2642 s; (f) 124.6 °C, 2774 s; (g) 124.6 °C, 2909 s; (h) 125.6 °C, 3780 s; (i) 126.6 °C, 4177 s; (j) 126.6 °C, 4377 s; (k) 127.6 °C, 5778 s; (h) 132 °C, 6638 s.

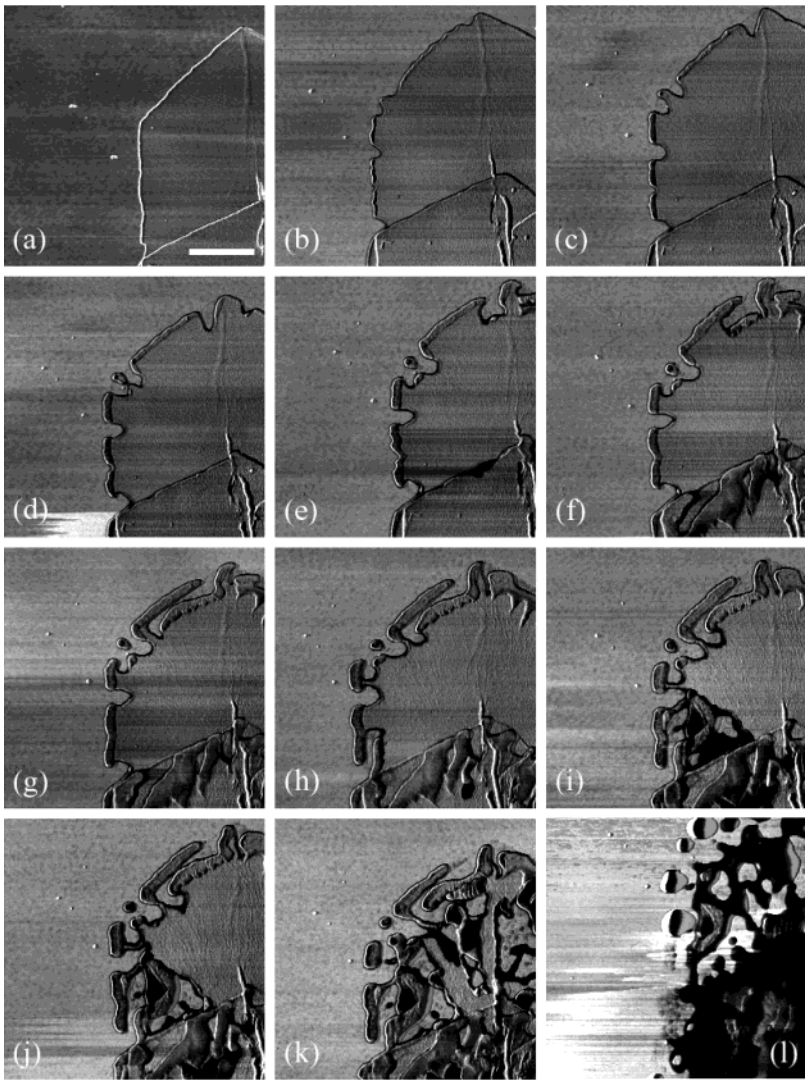

Figure 11. A series of AFM phase images collected simultaneously with the topographic images shown in Figure 10.

thickened material. Dark contrast in the phase image of this crystal (Figure 8e) shows that these areas are filled with molten material that subsequently crystallizes (Figure 8f) to leave a hole. Further large patches of molten material now start to appear and recrystallize in a thickened form. These can cover large areas of the crystal, while adjacent areas remain unchanged: note that molten material can be transported over significant distances before recrystallizing as a thickened rim on the edge of an unmelted section. During much of this process the overall crystal shape remains intact, as demonstrated by the ability to extract partially melted crystals from suspension in silicone oil. Eventually all the crystal thickens (Figures 7 and 8h) and then melts (Figures 7 and 8i).

Figure 4 showed an example of the morphological changes accompanying melting at a relatively high rate in the truncated lozenges, where preferential sector melting occurs. Here also the crystal edges have reorganized at an early stage in both the (110) and the (100) sectors, with the disruption of the (110) edges perhaps slightly more advanced. Figure 9 shows an example of truncated lozenge crystals heated to 124 °C at the lower rate of 2.5 °C min^{-1}. Chain reorganization is well advanced here: there are many examples of holes and thickened material within the crystals, while the overall shape remains largely preserved. No preferential sector melting has occurred. Fine lamellar structure is visible in some places, but it is apparent from the corresponding AFM images that this will have formed on cooling from patches of molten material which remain associated with the crystal even in suspension. No recognizable crystals could be recovered after heating to 126 °C, which corresponds to the end of the initial melting endotherm.

AFM pictures of truncated lozenges imaged during melting are shown in Figures 10 (topography) and 11 (phase). The initial thickening of the crystal edges is again clearly demonstrated in both sectors. By careful examination of the phase images, it is clear that thickening is always preceded by melting: even for this relatively small scale and localized rearrangement thickening would appear to proceed via melting and recrystallization rather than a solid-state thickening mechanism. Strips of thickened material, parallel to the growth front, are common [e.g., refs 5b and 10g]. The sequence of pictures in Figure 10e−h show clearly how these arise and provide one example of how thickening regions are "fed" from nearby areas of crystal. Another interesting feature illustrated in Figure 10 is the independent behavior of the overlying crystals at the bottom of the frame, where each crystal melts and thickens quite independently of the other. It had been suggested that overlying lamellae would be more prone

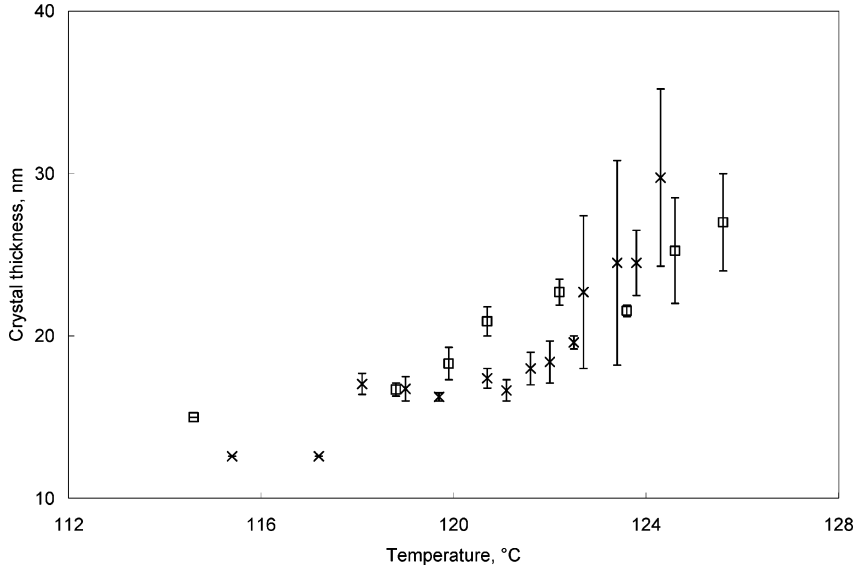

Figure 12. A graph showing the effect of temperature on crystal thickness of newly thickened material. Thicknesses are only of material that has formed from the next lowest temperature up to the temperature shown. The error bars indicate the range of different crystal thicknesses that are formed at that temperature; e.g., material that has thickened between 122.5 and 122.7 °C has thicknesses in the range 18−27.4 nm. The actual error in each thickness measurement is 1 nm. ×, Lozenge-shaped crystals; □, truncated lozenge crystals.

to thickening if a solid-state thickening mechanism were operating, as there would be a ready supply of material to fill the gaps left when one chain in a lattice extends. This is not borne out by the evidence here, which again supports a melting/recrystallization process. There may well be differences in behavior between overlying layers arising from multilayered crystals and those resulting from sedimentation, but this has not been explored here.

From the AFM micrographs we can measure the thickness of the material that has recrystallized/thickened at each temperature. These data are shown in Figure 12 for both lozenge and truncated lozenge crystals, the "error bars" showing the range of different thicknesses that are measured at each temperature for different thickened portions of the crystal, the actual error in thickness measurement being a constant for all measurements of approximately 1 nm. The AFM height measurements were obtained by taking a profile across the image from an area where the substrate was exposed to the thickened crystal. Height measurements were taken at each temperature of material that had not thickened at the previous temperature measured; i.e., if an image was taken at 120 °C and heights measured and then another image taken at 121 °C and heights measured, the latter heights were of material that had thickened between 120 and 121 °C. The greatest and smallest thickness of material formed at a particular temperature give the extent of the bars shown on the graph.

As can be seen, in both cases there is an overall trend toward thicker crystal as the temperature is increased, as expected. However, the range of different thicknesses that can be deposited is surprising. In particular, at around 123 °C in the lozenge crystals and 125 °C in the truncated crystals, large-scale melting and recrystallization begins, the recrystallized growth being in the range 25−35 nm. This is substantially thicker than that which occurred through more localized melting and recrystallization at the crystal edges (16−22 nm). It is this thicker material that is responsible for the final melting temperature measured with the DSC. At the same time that this thick material is being deposited,

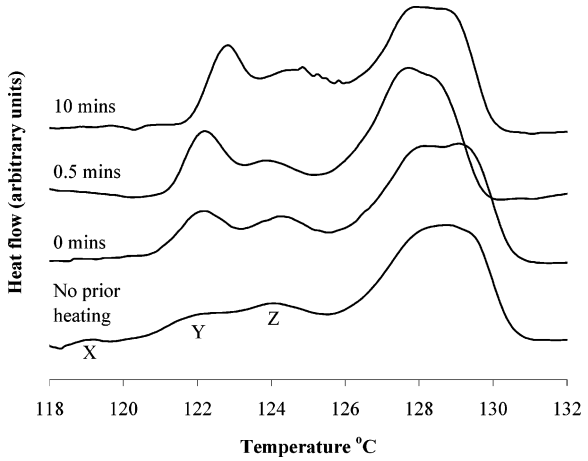

Figure 13. Melting endotherms obtained from lozenge-shaped crystals after annealing at 120 °C for the times shown.

some of the thickening is still occurring through local melting and still forming crystals with a thickness of around 24 nm. Thus, the crystal thickness that is formed during heating is controlled not only by the temperature at which it thickens but also by its local environment and the extent of the local melting that has occurred prior to thickening.

No consistent difference in melting point was observed between different types of crystal sector at the low heating rates used in the AFM. In the particular example shown in Figure 10, the (100) sector does eventually melt more quickly than the (110) sector (Figure 10i) but not until a late stage in the melting process.

Annealing Effects. Figures 13 and 14 show the effect on the subsequent melting behavior of annealing lozenge shaped crystals at various temperatures within the melting range. All samples were heated at 5 °C min^{-1}, and the melting trace obtained at this heating rate without any prior annealing is included in Figure 13 for comparison. For the nonannealed sample three primary melting peaks can be discerned: a very small peak at approximately 119.2 °C and two larger peaks

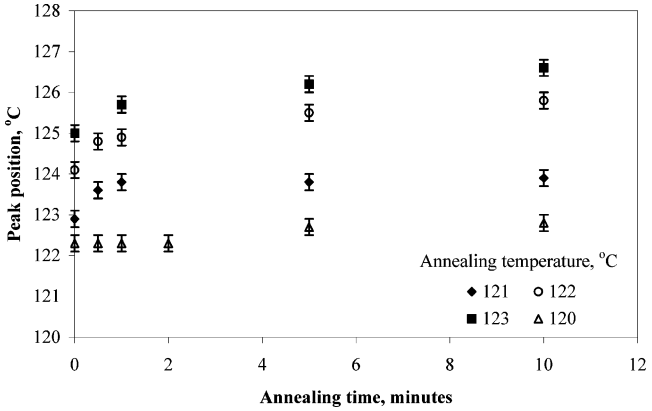

Figure 14. Melting endotherm peak positions as a function of time after annealing at the temperatures shown.

at approximately 122.2 and 124.2 °C. These peaks will be referred to as X, Y, and Z, as indicated in Figure 13. The annealing times refer to the period for which the sample was held at the annealing temperature, before cooling to 100 °C and subsequent reheating at 5 °C min^{-1}.

Figure 13 shows a selection of melting endotherms obtained after holding samples for various times at 120 °C, which is just above the very small peak X seen in the nonannealed sample. If the sample is simply heated to 120 °C and cooled, then the subsequent melting trace has only two peaks, and peak Y has grown considerably in proportion to Z. Holding the sample at 120 °C for 0.5 min further increases the relative height of peak Y, without any noticeable effect on the peak position. If the sample is held longer at 120 °C, then no additional increases in the height of peak Y are apparent, but the peak positions of both Y and Z shift to slightly higher temperatures.

Similar sets of melting endotherms were obtained for samples held at 121 °C (the onset of peak Y in the nonannealed sample), 122 °C (close to the peak position of peak Y in the nonannealed sample), and 123 °C (between peaks Y and Z in the nonannealed sample) for various times. The peak positions recorded during the final melting stage are shown as a function of annealing time in Figure 14. For the samples annealed at 121 °C a double melting peak was apparent but not clearly resolvable. The values plotted correspond to the lower temperature, higher intensity, portion of the peak. For samples annealed at 122 and 123 °C only one melting peak was obtained, and the Y, Z assignation is no longer appropriate. Peak Y values from Figure 13 have also been included for comparison.

The main point to note here is the contrast between the very small and slow changes to the peak positions at the lowest annealing temperature and the more pronounced, rapid and continuous changes seen at higher temperatures. The behavior at 121 °C is intermediate: a rapid initial increase in peak position that then stabilizes.

Discussion

By combining observations from three different techniques, TEM, DSC, and AFM, it is possible to identify different stages of reorganization in these crystals, which occur at successively higher temperatures.

(a) An initial local reorganization within the crystals, which takes place several degrees below the apparent onset of melting. This reorganization is not directly visible using any of the techniques employed here, although the AFM did reveal some distortion to the crystal outline prior to melting. It can be deduced from changes in the subsequent melting behavior, such as the disappearance of preferential sector melting, after slow heating or suitable annealing.

(b) Small scale melting and recrystallization around the edges of individual crystals, which is finite in extent and does not progress into the bulk of the crystal over the time scales used in these experiments. Individual crystals remain recognizable. This is not attributable to a thinner rim round the edges of the crystals: the hot filtration and washing employed during the initial crystallization make this unlikely, and there was no evidence from either TEM or AFM of any thinner rim.

(c) Larger scale melting and recrystallization in the bulk of the crystals, which produces a progressive increase in crystal thickness/melting point over time. Original crystal habits are eventually lost.

(d) Final melting of the thickened crystals produced in (c).

The preferential sector melting which provided one focus for this study was not consistently observed at the low heating rates required for AFM imaging, nor after holding crystals at a temperature just below the visible onset of melting. This indicates that a change is taking place within the crystals at temperatures a few degrees below the visible onset of melting, over a time scale of several minutes, which affects the two types of sectors differently. No change in the thickness of the crystals is detected but the crystal edges begin to distort, suggesting reorganization within the crystal possibly driven by a relaxation of strain in the lattice.

A previous study of preferential sector melting in polyethylene single crystals found that the effect was most pronounced when the (100) sectors were relatively small. The separation between the two melting peaks ΔT_m decreased, and eventually disappeared completely, as the axial ratio increased from 1.6 to 3.0.[13] In that case slight variations in crystal thickness between sectors or differences in the surface free energy arising from a higher work of folding along (100) were postulated. Neither of these explanations seems consistent with the present finding that the difference in melting point can be annealed out before melting without any significant visible change in the crystals.

Recent studies of unfolding transitions in long *n*-alkanes have revealed very small differences in lattice spacing in crystals containing different numbers of folds.[22] It therefore seems plausible that the specific heat of fusion, ΔH, is affected by the nature of the fold in different crystal sectors. The relative growth rate of the (110) and (100) faces, G_{110}/G_{100}, can be calculated from the axial ratio of polyethylene crystals.[9] As the relative size of the (100) sectors increases, the overall growth rate is slower but the ratio G_{110}/G_{100} increases. The changes in ΔT_m with axial ratio can be explained if we assume that the degree of order in the (100) sectors improves as the growth rate decreases. A similar effect could be achieved by annealing at, or heating slowly through, temperatures just below the melting point, as observed here.

In addition to any small differences in lattice spacing between sectors there will be a gradual thermal expansion as the crystals are heated. This thermal expansion is slightly different in different crystallographic directions.[22] This will introduce strain into the lattice and

could be responsible for the shape distortions seen in the AFM just before the onset of melting.

Moving on to consider melting around the crystal edges, the most surprising feature of this stage of the process is that it appears quite self-contained. During the AFM studies crystals were held at this stage for quite prolonged periods, but the melting remained restricted to the edges until the temperature was raised. This is backed up by the DSC results in Figure 13. Heating to 120 °C causes a change in subsequent melting behavior, but after the initial change there is very little further development and only a very small shift in the position of the melting peak.

Crystal edges may melt more easily for reasons connected with energy and/or chain mobility. The chains at the edge of the crystal will be less tightly bound within the lattice and could rearrange to give a thicker, more thermodynamically stable crystal that would then provide a barrier to further thickening. The morphological evidence does not support this proposition: there is no continuous rim of thickened material around the edges that would block further thickening. An alternative explanation may lie in the lattice strain which we have suggested results from differential thermal expansion within the crystal. As the temperature is increased and the chains become more mobile, the strain in the lattice can be relieved by small scale movements of chains at the crystal edges which may initiate localized melting and recrystallization. The rearrangement would stop once the driving force provided by the strain had been sufficiently reduced. The edges of the lozenge-shaped crystals in Figure 6a appear serrated in a crystallographic manner: such morphology could arise if the chains had adjusted their positions to accommodate differential thermal expansion while relatively mobile at high temperature and then been rapidly cooled.

It is well-known that the melting temperature of a polymer can be affected by annealing and will increase with both temperature and time of annealing. Such behavior is seen here at temperatures above 121 °C. Once thickening has progressed into the main body of the crystal it progresses rapidly, and material that has already thickened can thicken further. The AFM images show that melting occurs in patches, from which material travels to a nearby thickening region, and that overlapping crystal areas can behave independently. There is no clear evidence to suggest whether the continued progressive thickening occurs via a secondary melting/recrystallization process or by solid-state rearrangement. The mobility of the chains at these elevated temperatures is likely to be very high, so the distinction between the two may well be hard to define.

It is interesting to compare our observations with results from other recent AFM studies of polyethylene single-crystal melting and annealing, carried out under different experimental conditions. Tian and Loos[16] see very similar effects at the edges of slightly truncated lozenge-shaped crystals deposited on mica in the early stages of melting and only very slight indications of preferential sector melting, in line with our results. Magonov et al.[15] compared the behavior of "wet" and "dry" crystals of polyethylene and a long alkane on graphite or silicon substrates. The polyethylene crystals were truncated lozenge shaped but were not grown isothermally. The initial edge melting was not apparent in these samples—instead, small holes appeared all over the surface of the crystal which were later surrounded by a rim of thickened material. Hocquet et al.[17] use several techniques in combination with AFM in a study of morphology and melting of truncated crystals, which concentrates on variations in crystal thickness during thickening and melting. They observe preferential sector melting in the AFM under different heating conditions to those used here and measure a difference in the thickness of the two sectors that is attributed to chain tilt. Factors such as thermal history, molecular weight, crystal size and shape, and substrate are all likely to be factors in determining melting behavior, and we do not wish to speculate on the reasons for these differences. We note, however, that using the experimental setup utilized in the present study, it has been possible to image continuously during heating, with no stepwise changes in temperature, and this may explain some of the differences in the observed behavior.

Conclusion

The combination of AFM with DSC and TEM provides a powerful means of correlating thermal measurements from the bulk sample with morphological changes in individual crystals and has provided us with new insights into the different processes involved in melting and recrystallization. We have examined different stages in the melting of polyethylene single crystals and found that the extent to which these take place depends to some extent on the heating conditions employed.

Melting is preceded by local reorganization within the crystals which we believe leads to perfectioning of the crystal lattice. The most obvious manifestation of this is the disappearance of preferential sector melting in truncated lozenge crystals that have either been heated slowly to their melting point or annealed at temperatures just below the melting point prior to melting. The extent to which this takes place depends crucially on the thermal history of the sample.

The first visible signs of melting occur at the edges of the crystals and are preceded by distortions in crystal shape observed by AFM. Small scale melting occurs, and thickened portions are nucleated around the edges of the crystals. Crystals quenched at this stage often have distinct serrated edges which we have attributed to release of lattice strain arising from differential thermal expansion. The edge thickening is self-contained and did not extend further into the crystals over the time scales used in these experiments.

The next step in the melting process is larger scale melting and recrystallization within the bulk of the crystal, which leads to a progressive increase in melting point. The melting is quite patchy, and material can travel over appreciable distances within the crystal before recrystallizing in a thickened form. There is no evidence for any solid-state reorganization, and overlying layers can behave quite independently. These thickened crystals eventually melt, with a final melting point dependent on the thermal history of the sample. This behavior is well documented in bulk polymers.

References and Notes

(1) Frank, F. C.; Tosi, M. *Proc. R. Soc. London A* **1961**, *263*, 323.
(2) Peterlin, A. *J. Appl. Phys.* **1960**, *31*, 1934.
(3) Muthukumar, M. *Philos. Trans. R. Soc. London A* **2003**, *361*, 539.
(4) Sadler, D. M.; Spells, S. J. *Macromolecules* **1989**, *22*, 3941.
(5) Sommer, J. U.; Reiter, G. *Europhys. Lett.* **2001**, *56*, 755.
(6) Toda, A.; Hikosaka, M.; Yamada, K. *Polymer* **2002**, *43*, 1667.

(7) Keller, A.; Hikosaka, M.; Rastogi, S.; Toda, A.; Barham, P. J.; Goldbeck-Wood, G. *J. Mater. Sci.* **1994**, *29*, 2579.
(8) Strobl, G. *Eur. Phys. J. E* **2000**, *3*, 165.
(9) Organ, S. J.; Keller, A. *J. Mater. Sci.* **1985**, *20*, 1571.
(10) Bassett and Keller sector melting.
(11) Geil, P. H. *Polymer Single Crystals*; Wiley/Interscience: New York, 1963.
(12) Harrison, I. R. *J. Polym. Sci., Phys.* **1973**, *11*, 991.
(13) Organ, S. J.; Keller, A. *J. Mater. Sci.* **1985**, *20*, 1586.
(14) Alfonso, G. C.; Ceschina, M.; Chiappa, V.; Pedemonte, E. In *Crystallization of Polymers;* Dosiere, M., Ed.; *NATO ASI Ser. C: Math. Phys. Sci.* **1993**, *405*, 81.
(15) Maganov, S. N.; Yerina, N. A.; Ungar, G.; Reneker, D. H.; Ivanov, D. A. *Macromolecules* **2003**, *36*, 5637.
(16) Loos, J.; Tian, T. *e-Polym.* **2002**, *36*, 1.
(17) Hocquet, S.; Dosiere, M.; Thierry, A.; Lotz, B.; Koch, M. H. J.; Dubreeuil, N.; Ivanov, D. A. *Macromolecules* **2003**, *36*, 8376.
(18) Winkel, A. K.; Hobbs, J. K.; Miles, M. J. *Polymer* **2000**, *41*, 8791.
(19) Blundell, D. J.; Keller, A.; Kovacs, A. J. *Polym. Lett.* **1966**, *4*, 481.
(20) Wittmann, J. C.; Lotz, B. *J. Polym. Sci., Polym. Phys. Ed.* **1985**, *23*, 205.
(21) Hobbs, J. K.; Humphris, A. D. L.; Miles, M. J. *Macromolecules* **2001**, *34*, 5508.
(22) Terry, A. E.; Phillips, T. L.; Hobbs, J. K. *Macromolecules* **2003**, *36*, 3240.

MA035955R